



Contents lists available at ScienceDirect

Journal of Alloys and Compounds

journal homepage: <http://www.elsevier.com/locate/jalcom>Experimental and *ab initio* study of the Ag–Li system for energy storage and high-temperature soldersM.H. Braga ^{a,*}, A. Dębski ^{b,**}, S. Terlicka ^b, W. Gąsior ^b, A. Góral ^b^a LAETA, Engineering Physics Department, FEUP, University of Porto, R. Dr. Roberto Frias s/n, 4200-465, Porto, Portugal^b Institute of Metallurgy and Materials Science, Polish Academy of Sciences, 30-059, Kraków, 25, Reymonta Street, Poland

ARTICLE INFO

Article history:

Received 30 August 2019

Received in revised form

22 October 2019

Accepted 25 October 2019

Available online xxx

Keywords:

Intermetallics

Enthalpy

Thermodynamic properties

Calorimetry

Thermodynamic modeling

X-ray diffraction

ABSTRACT

The standard enthalpies of formation of the $\text{Ag}_{30}\text{Li}_{70}$ and $\text{Ag}_{20}\text{Li}_{80}$ gamma phases (cubic, sg. I-43 m) were measured using the solution calorimetry method; the standard enthalpy of formation of the $\text{Ag}_{10}\text{Li}_{90}$ alloy, corresponding to a hypothetical γ phase, was determined using the same method. All the measured and literature values of the standard enthalpies of formation of the Ag–Li intermetallic phases were compared with the data calculated using *ab initio* for stable and unstable phases and Miedema's model. The XRD pattern for a sample with $\text{Ag}_{30}\text{Li}_{70}$ was obtained and it was verified that it contained the γ phase, as expected. Moreover, the structure of the γ -phase for the Ag_4Li_9 disordered phase was minimized and the vibrational heat capacity at constant volume and the thermal coefficient of linear expansion were calculated using *ab initio* methods. The simulated XRD pattern of the latter phase was compared with the experimental pattern. It was determined that only one gamma phase, with a homogeneity range not wider than $0.69 \leq x(\text{Li}) \leq 0.73$, is stable for $T \geq 298$ K. Furthermore, besides $\text{AgLi}-\beta$ with a homogeneity range of $0.50 \leq x(\text{Li}) \leq 0.60$ at 298 K, a cubic $\text{Ag}_{15}\text{Li}_{49}-\beta$ is stable for $x(\text{Li}) = 0.77$. The entropy term stabilizes the cubic structure of the $\text{AgLi}-\beta$ which can be tetragonal at 298 K. The enthalpies and Gibbs energies of formation were calculated at 298, 320, 425, and 600 K. A new “map” of the phases in equilibrium at different temperatures is proposed.

© 2019 Elsevier B.V. All rights reserved.

1. Introduction

The 21st century has been characterized by a scientific search for new ecological fuels for the automotive industry. Alternative energy sources for electronic devices and new soldering materials for electronics have, therefore, been a research target.

Although the Ag–Li alloys have been developed as materials for energy storage and to produce high-temperature solders used in vacuum brazing, their thermodynamic properties and phase diagram data are limited. The reason for this is probably the high reactivity of lithium at elevated temperature with the air contained elements (O_2 , N_2 , H_2O) and the high energy effects accompanying the respective reactions. Moreover, liquid lithium reacts readily with the ceramic elements of the apparatus used for investigations and preparation of alloys and this is another barrier limiting the studies of Li-containing alloys.

The phase diagram of the Ag–Li system presented in the literature was assessed by Freeth and Raynor in 1954 [1] based on the thermal and X-ray analysis of the alloys prepared from high purity Ag and Li. The latter authors did not consider Pastorello's [2,3] earlier results obtained using the same methods and which pointed to the existence of two intermetallic phases, AgLi and AgLi_3 , which melted incongruently at 723 K and 955 K, respectively. In contrast, Freeth and Raynor [1] based on their experimental data and microstructure of solid alloys suggested three γ -brass alloys (γ_1 , γ_2 , γ_3) with a homogeneity region instead of the AgLi and AgLi_3 proposed by Pastorello [2,3]. The phase diagram proposed by Okamoto [4] was almost identical to Freeth and Raynor's [1] phase diagram.

The structure of the silver solid solutions (Ag)- α was investigated by Perlitz [5] and the lattice parameters determined by Firth et al. [6] and by Kelington et al. [7]. The short-range order parameters in the Ag–Li alloys were investigated by Ruppertsberg [8] and Migge and Andersen [9]. Moreover, the structure of the γ_3 and γ_2 phases was studied by Arnberg and Westman [10,11] and Noritake and co-workers [12].

The first experimental thermodynamic studies of the Ag–Li

* Corresponding author.

** Corresponding author.

E-mail addresses: mbraga@fe.up.pt (M.H. Braga), a.debski@imim.pl (A. Dębski).

alloys were conducted by Predel et al., in 1979 [13]; they measured the enthalpy of mixing of the liquid and solid solutions. Predel et al. [13] conducted studies at 1250 K for the liquid solutions in the entire range of concentrations and for solid alloys between 0 and 0.55 mol fraction of Li at 623 K. Becker et al. [14] performed an electromotive force (EMF) study for the liquid phase at 823 K.

In 1986, Pelton [15] presented a Ag–Li phase diagram where liquidus and solidus were calculated based on calorimetric measurements [13] and the assumption that the liquid and solid (Ag)– α alloys are regular solutions. Nonetheless, Pelton [15] did not obtain a thermodynamic assessment of the phase diagram and, therefore, the other equilibrium lines were not calculated.

Due to the very limited number of experiments on the thermodynamics of the Ag–Li alloys we have decided to undertake experiments on calorimetry for the liquid [16] and solid [17] alloys, EMF [18] and dilatometry studies [19].

Recently, the tetragonal AgLi phase sg. I41/amd was found to be more stable than the cubic sg. Pm-3m (β -phase) at room temperature by Ref. [20], which was also confirmed by Refs. [17,19]; the correspondent crystal structure parameters were obtained after structure optimization using first principles.

In 2015, Wang et al. assessed the phase diagram based on the available experimental data [21]. Okamoto republished Wang et al. phase diagram in 2017 [22].

Here we study the Ag–Li system using first-principles calculations. The crystal structures are optimized using random substitution, special quasirandom structure (SQS), or substitutional search, depending on the type of structure (e.g. fcc or bcc), and finally by performing *ab initio* calculations. We calculate the lattice parameters, X-ray diffraction (XRD) patterns, thermal coefficients of linear expansion, enthalpy and Gibbs energies of formation of the solid Ag–Li phases and determine which structures and stoichiometries are stable and what are the equilibria at different temperatures. Furthermore, we compare the first-principles calculations of the enthalpy of formation with the calculated using the Miedema model [23].

Calorimetric studies to determine the enthalpies of formation of the $\text{Ag}_{30}\text{Li}_{70}$ (γ_3) and $\text{Ag}_{20}\text{Li}_{80}$ (γ_2) phases, and the $\text{Ag}_{10}\text{Li}_{90}$ (γ_1) alloy were performed.

To determine the crystal structure of $\text{Ag}_{30}\text{Li}_{70}$, XRD experimental data were obtained and compared with the calculated.

2. Material and methods

To establish the enthalpy formation of the intermetallic phases of the Ag–Li system, metallic silver (purity 99.9 wt.% Innovator Sp. z o.o.) and lithium (Alfa Aesar purity 99.9 wt.%) were used. The intermetallic γ phases with 70 at.% Li, 80 at.% Li and an alloy with a composition of approximately 90 at.% Li (hypothetical γ_1 phase [1]) were prepared from weighed amounts of metals at 673 K in a glove box with a protective atmosphere constituted by high purity argon ($\text{H}_2\text{O} < 0.5$ ppm, $\text{O}_2 < 0.1$ ppm). The nitrogen concentration was not recorded; however, the nitrogen was removed from the argon by making titanium react at 1200 K inside the N_2 -absorber connected to the glove box. The weighed metals were melted in heat resistant steel (H25T) crucibles. The pure Li and the samples of the Ag–Li system were held in the glove box after being produced to avoid reactions with the components of the air; immediately before the measurements, the samples were removed from the glove box into the calorimeter in a tight delivery device that was filled with the crucibles inside the glove box.

The structural studies of the prepared alloys were conducted using a D2 Phaser (Bruker, Cu K α radiation) diffractometer. The analysis of the phases was performed with the Diffrac. EVA software. The diffraction pattern of the sample with 70 at.% Li is shown

in Fig. 1.

The studies of the enthalpies of formation of the gamma phases γ_3 , γ_2 , and γ_1 in Ref. [1] corresponding to $\text{Ag}_{30}\text{Li}_{70}$, $\text{Ag}_{20}\text{Li}_{80}$, and the $\text{Ag}_{10}\text{Li}_{90}$ alloys were conducted by solution calorimetry method, which was described in our previous publications [24,25] and were performed using the Setaram MHTC 96 Line evo calorimeter.

The enthalpy of formation ($\Delta_f H$) of the phases here considered, determined by this method, was obtained from the difference of

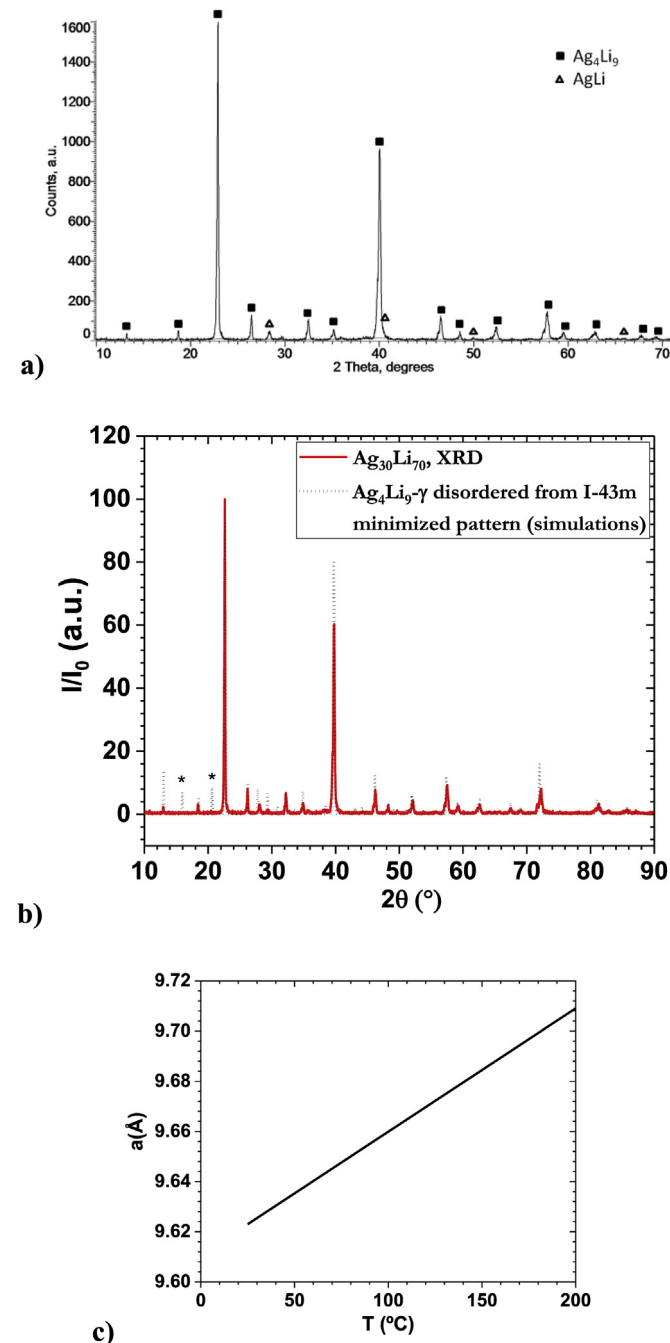


Fig. 1. X-ray diffraction pattern of a sample containing $\text{Ag}_{30}\text{Li}_{70}$ (CuK α radiation) at room temperature; **a)** XRD experimental pattern matched with Ag_4Li_9 - γ (cubic, space group n. 217, I-43 m) and AgLi- β (cubic, space group n. 221, Pm-3m) phases; **b)** XRD experimental pattern superimposed to calculated Ag_4Li_9 - γ obtained from cubic, space group n. 217, I-43 m disordered phase (*peaks from the Ag_4Li_9 - γ calculated pattern that were not identified in the experimental pattern); **c)** lattice parameter vs temperature using the thermal linear expansion coefficient in Table 1.

the heat effects accompanying the dissolution of the studied phases and their components in the Sn bath. For calculations, the following equation was applied:

$$\Delta_f H = x_{Ag} \Delta H_{Ag}^0 + x_{Li} \Delta H_{Li}^0 - \Delta H_{x_{Ag}x_{Li}}^0 \quad (1)$$

where $\Delta_f H$ is the enthalpy of formation of a certain phase, x_{Ag} , x_{Li} are the concentrations (mole fractions) of the components, ΔH_{Ag}^0 , ΔH_{Li}^0 , $\Delta H_{x_{Ag}x_{Li}}^0$ are the heat effects accompanying the dissolution of the components and the phase in the Sn bath.

3. Calculations

3.1. First-principles calculations

One of the most important methods of quantum mechanical modeling of solids is the framework of Density Functional Theory (DFT) [26] using the Generalized Gradient Approximation (GGA) [27].

DFT calculations with Projector Augmented Wave (PAW) pseudopotentials [28], and the Perdew–Burke–Ernzerhof (PBE) functional [29] were used as implemented in the Vienna Ab Initio Simulation Package (VASP) code [30]. A plane wave cut-off of at least 400.00 eV and k-spacings of $0.230 \times 0.230 \times 0.230 \text{ \AA}^{-1}$ were used. Calculations were performed in the real and reciprocal space and for a broad range of phases of the Ag–Li phase diagram. Each phase was calculated for different space groups; when applicable, each phase was optimized with a structure and stoichiometry as close as possible to the corresponding published versions. The total energy was minimized with respect to the volume (volume relaxation), the shape of the unit cell (external relaxation), and the position of the atoms within the cell (internal relaxation). The MT module as implemented in Materials Design [31] was used to calculate the thermal coefficient of linear expansion, enthalpies and Gibbs energies of formation which were compared with the ones obtained with Phonon [32].

The phonon direct method [32] was applied to predict the lattice dynamics using the harmonic approximation in VASP's minimized structures that had the lowest ground state energy. Therefore, the electronic structure at the ground state and the zero-point energy was calculated using VASP, while the phonons' energy and the entropy were calculated using Phonon. In fact, we have calculated the Helmholtz free energy, which can be approximated to the Gibbs free energy at zero stress.

The Helmholtz free energy, the internal energy which can be approximated to the enthalpy, and the entropy were calculated after the vibration frequencies, ω , as follows:

$$F_{\text{phonon}} = 3Nk_B T \int_0^{\omega_L} \ln \left(2 \sinh \frac{\hbar \omega}{2k_B T} \right) g(\omega) d\omega \quad (2)$$

$$E_{\text{phonon}} = 3N \frac{\hbar}{2} \int_0^{\omega_L} \omega \coth \left(\frac{\hbar \omega}{2k_B T} \right) g(\omega) d\omega \quad (3)$$

$$S_{\text{phonon}} = 3Nk_B \int_0^{\omega_L} \left[\frac{\hbar \omega}{2k_B T} \coth \left(\frac{\hbar \omega}{2k_B T} \right) - \ln \left(2 \sinh \frac{\hbar \omega}{2k_B T} \right) \right] g(\omega) d\omega \quad (4)$$

where N is the number of atoms in the cell, k_B is Boltzmann's constant, T the absolute temperature, ω_L the maximal frequency and $g(\omega)$ the frequency distribution function. Therefore, adding the

electronic contribution, E_{elec} , calculated using DFT as implemented in VASP, the ZPE zero-point energy of the quantum harmonic oscillator, $E(0 \text{ K}) = \frac{1}{2} \hbar \omega$, plus the phonon contribution (calculated using phonon) defines $E(T) = E_{\text{elec}} + \text{ZPE} + E_{\text{phonon}}(T)$. The Helmholtz free energy, $F(T)$, is given by $F(T) = E(T) - TS(T)$ in which $S(T) = S_{\text{phonon}}(T)$ is the vibrational entropy at the absolute temperature T . The Helmholtz free energy was assumed to be equal to the Gibbs free energy since the variation of the PV term (in which P is the pressure and V the volume) can be neglected for solids under no applied stress.

4. Results and discussion

The crystal structure of a sample containing $\text{Ag}_{30}\text{Li}_{70}$ was studied to determine the structure of the gamma phase, γ_3 in Ref. [11] as shown in Fig. 1. The lattice parameters obtained in this study and in Ref. [11] are shown in Table 1 for comparison.

As observed in Fig. 1, the XRD pattern of the sample can be fully described by a slightly distorted and disordered gamma phase that evolves from the cubic I-43 m crystal structure. We highlight that since this phase is disordered and there is a limitation on the number of atoms that can run in a calculation, the XRD pattern is not univocal. The latter should be considered when comparing calculated with experimental XRD patterns. Moreover, anisotropy is likely to exist in the experimental sample justifying the difference in peaks' intensities, especially at low angles. For $2\theta > 35^\circ$ the pattern is well matched just by superimposing and correcting the experimental pattern with a zero shift of $2\theta = -0.28^\circ$. Furthermore, if the experimental XRD pattern is matched to the gamma phase, γ_3 , as obtained in Ref. [11], then the remaining peaks can be justified by the presence of small amounts of the AgLi- β intermetallic phase (CsCl type structure - two sublattices, body-centered, Pm-3m) [1]. The small amount of the β -phase in the sample should not significantly influence the value of the measured heat effect of the solution but according to our first-principles calculations, the gamma and beta disordered phases, stable in homogeneity ranges, distort into tetragonal structures at low temperatures. This phenomenon was observed experimentally in XRD studies [17,19,20].

Fig. 1a and b, 2 and Table 1 show additional results for Ag_4Li_9 - γ disordered phase; the lattice parameter, the vibrational heat capacity at constant volume, and the thermal linear expansion coefficient vs temperature and the Debye temperature are shown.

In the case of γ_2 -phase and γ_1 -phase (alloy close to composition 90 at.% Li) [1], the X-ray diffraction patterns were not available and first-principles calculations data do not envisage the existence of three gamma-phases as will be described further in this text.

The measurements of the limiting enthalpy of solution of Ag in liquid Sn and Li in liquid Sn were taken from our earlier work [24,33]. The necessary thermodynamic data of the metals used in

Table 1

Comparison between the lattice parameters obtained for Ag_4Li_9 in this work (experimental and *ab initio*) and in the literature. In the *ab initio* optimization, no constraints were imposed; atom positions, volume, and shape were free to vary since the structure is disordered. The thermal linear expansion coefficient, α , was averaged between $298 \leq T(\text{K}) \leq 475$ for the calculated values in Fig. 2b.

Phase	Lattice parameter [Å]			Reference
	a	b	c	
Ag₄Li₉ cubic I-43 m	9.602	9.602	9.602	[11]
	9.523	9.523	9.523	This study (exp)
	9.578	9.645	9.645	This study (<i>ab initio</i>) (slightly tetragonal)
	9.623			(average)
$\alpha = (51 \pm 1) \times 10^{-6} \text{ K}^{-1}$				$298 \leq T(\text{K}) \leq 475$

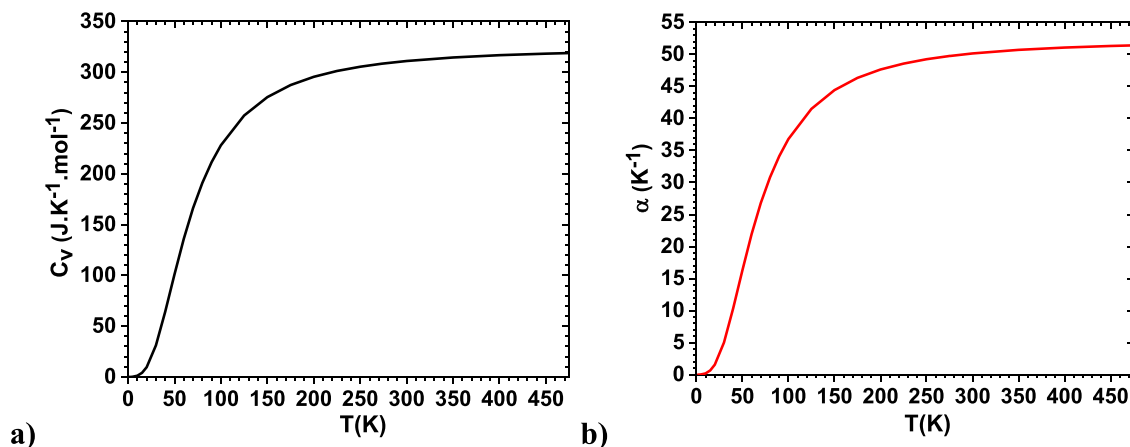


Fig. 2. Thermodynamic data for the $\text{Ag}_4\text{Li}_9\text{-}\gamma$ disordered phase (cubic, space group n. 217, I-43 m) calculated using *ab initio* methods as implemented in Refs. [30–32] for temperatures below the melting point $T < T_m$; **a)** vibrational heat capacity at constant volume and **b)** thermal linear expansion coefficient vs temperature calculated using the MT module of [31]; Debye temperature: 275.7 K.

the calculations were obtained in Ref. [34].

The determination of the standard enthalpy of formation was conducted considering identified intermetallic phases and the results obtained are presented in Table 2 and in Fig. 3; in Fig. 3 the enthalpies of formation are compared with similar data available in the literature. The results obtained with this study are in good agreement with those available in the literature [13,17] but none agree with the calculated results obtained by first principles and using Miedema's model, demonstrating the difficulty associated with the measurement of the thermodynamic properties of this system, as discussed above, and the importance of *ab initio* calculations. The difference between experimental [17] and calculated enthalpies of formation overcomes 10 kJ mol^{-1} . The calculation of the electronic energy of formation of AgLi tetragonal (solid solution with two sublattices) in Fig. 4, represented by star (1), might give a hint for what is happening experimentally; it is possible that the alloys' synthesis does not fully allow equilibration and the formation of ordered phases such as the AgLi- β intermetallic cubic phase (CsCl type structure - two sublattices, body-centered, Pm-3m)

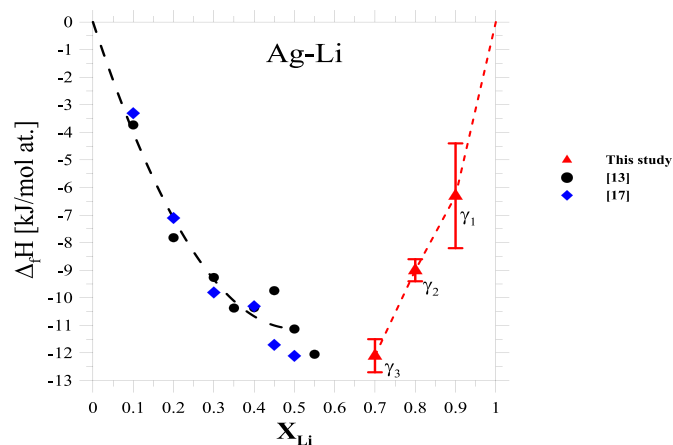


Fig. 3. Enthalpy of formation of the Ag–Li intermetallic phases. Integral molar enthalpies of solid Ag–Li alloys taken from Refs. [13,17].

Table 2

Heat effects ΔH^{eff} and enthalpies of formation $\Delta_f H$ of intermetallic phases of the Ag–Li system. The temperature of the Sn bath was 723 K.

Phases	T [K]	No of sample	ΔH^{eff} [kJ/mol at.]	$\Delta_f H$ [kJ/mol at.]
Ag ₃₀ Li ₇₀	298	1	–9.3	–12.7
		2	–10.5	–11.5
		3	–9.5	–12.5
		4	–9.8	–12.1
		5	–9.3	–12.7
		6	–10.6	–11.4
		Average	–9.8	–12.1
Ag ₂₀ Li ₈₀	298	Standard deviation	0.6	0.6
		1	–19.9	–8.9
		2	–20.3	–8.5
		3	–19.2	–9.6
		4	–20.1	–8.7
		5	–19.4	–9.4
		6	–19.7	–9.1
Ag ₁₀ Li ₉₀	298	Average	–19.8	–9.0
		Standard deviation	0.4	0.4
		1	–26.7	–8.9
		2	–29.1	–6.5
		3	–31.1	–4.5
		4	–30.2	–5.4
		Average	–29.3	–6.3
		Standard deviation	1.9	1.9

stable at and above room temperature [1]. Furthermore, the analysis of Figs. 4–6 shows how important the entropy term of the Gibbs energy of formation is, especially at $x(\text{Li}) = 0.5$; without considering the entropy term, AgLi- β is not stable. In fact, AgLi is stable at 298 K and it increases stability as the temperature increases; these observations are corroborated by the XRD results obtained by Refs. [17,19,20]. In this study, although the tetragonal structures for the β phase are found to be stable at lower temperatures, they do not have a space group I41/amd as reported in Ref. [20].

The experimental data of the standard enthalpies of formation are shown with the calculated data (first-principles study and Miedema's model) in Table 3 and Fig. 4.

The electronic energy of formation, E_f , which corresponds to VASP's energy of formation, is shown in Fig. 4. Additional structures were calculated, and their stability checked with caution since, as we have highlighted before, the entropy term is important in this system. We have ruled out numerous structures that were obtained by making Li occupying a sublattice in the fcc structure (Ag); those structures had positive E_f .

Fig. 4b shows the E_f curves vs $x(\text{Li})$ in stable and unstable regions of the phase diagram. Each curve was obtained by curve fitting the data to second-order polynomials, except the β -phase data that was

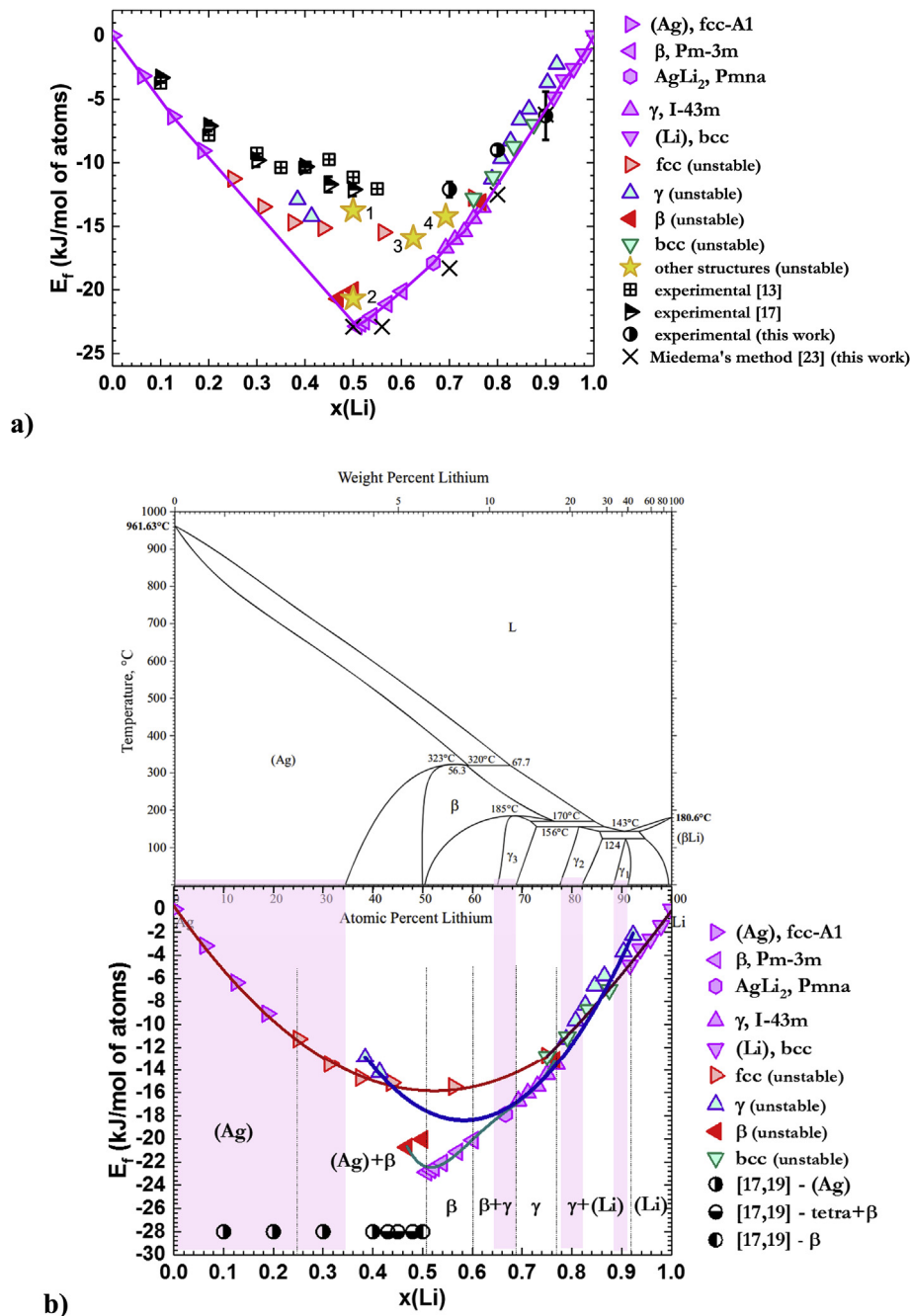


Fig. 4. Electronic energy of formation (VASP's energy of formation) for stable and unstable phases of the Ag–Li system; **a)** E_f is approximated to $\Delta_f H = \Delta_f G(0\text{ K})$ and results are compared with available experimental and Miedema's calculated data; in this approximation the zero-point energy is not considered; stars: 1-AgLi, tetragonal (solid solution with 2 sublattices), 2-AgLi, tetragonal s.g. I41/amd [20], 3-Li₉Ag₄, cubic sg. P-43 m, 4-Li₅Ag₃, hexagonal; **b)** $\Delta_f G(0\text{ K})$ vs lithium concentration curves determining phase equilibria at 0 K.

fitted to a fourth-order polynomial. Considering $E_f \approx \Delta_f G(0\text{ K})$, observing the convex hull in Fig. 4a, the curves and double tangents (not signaled) in Fig. 4b, the stable phases in the phase diagram were determined at 0 K. This exercise conducted us to the following observations, 1- the E_f vs $x(\text{Li})$ curve correspondent to (Ag)- α , fcc-A1, shows the same energy in the unstable region (Li-rich region) as the (Li)- β , bcc-A2, stable phase, and vice-versa; 2- β and γ have very similar energies, E_f , for $0.68 \leq x(\text{Li}) \leq 0.75$.

According to our calculations, the solvus line, separating (Ag) from (Ag) + β regions, crosses the concentration axis at $x(\text{Li}) = 0.25$ at low temperature, but experimental results in Ref. [19] show that the solvus line only crosses the concentration

axis at $x(\text{Li}) \approx 0.40$. As mentioned previously, we have calculated numerous structures with $0.25 \leq x(\text{Li}) \leq 0.4$ and we could not find any stable phases in this region. The most stable structures for (Ag) in the $0.25 \leq x(\text{Li}) \leq 0.4$ range, shown in Figs. 4–6, were obtained by minimizing the electronic energy starting from a face-centered cubic structure using the special quasi-random structure (SQS) method. We highlight that the (Ag) + β region is certainly wider than firstly proposed by Freeth and Reynor [1] and likely even wider than proposed by Wang et al. [21] (Fig. 4b). The other differences observed are related to the γ -phase. We did not observe more than one gamma phase; this gamma phase has a wider homogeneity range than any gamma phase proposed by Freeth and

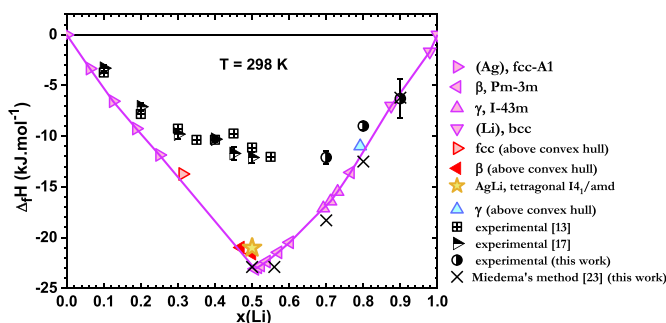


Fig. 5. Experimental, first principles and Miedema's model [23] data for the enthalpies of formation of the solid phases in the Ag–Li system. The calculations of the enthalpy of formation had into account the electronic plus vibrational energy of formation and the enthalpies were calculated at 298 K.

Reynor [1] and recently by Wang et al. [21] (adapted by Okamoto [22]) (Fig. 4b). The γ -phase homogeneity range is $0.69 \leq x(\text{Li}) \leq 0.77$ at 0 K.

According to this study, the β -phase is stable between $0.5 \leq \text{AgLi-}\beta \leq 0.6$ and again at $x(\text{Li}) = 0.77$ and 298 K. The latter phase is stabilised by the entropy term as demonstrated by the comparison of Figs. 4 and 6. Phase β , $\text{Ag}_{15}\text{Li}_{49}$, is represented by a full dot in Fig. 6

and was optimized from a cubic sg, Pm-3m structure. Fig. 7 shows the XRD calculated patterns of $\text{Ag}_{15}\text{Li}_{49}$ - β and $\text{Ag}_3\text{Li}_{10}$ - γ disordered phases with comparable concentrations of lithium. If an XRD pattern is obtained experimentally for $2\theta > 25^\circ$ it is very difficult to distinguish between β and γ phases since the most intense peak is superimposed in both structures and each of these phases is likely to show structural anisotropy; moreover, other phases may coexist in the same pattern with makes it more difficult to distinguish between the two phases. The lithium-rich gamma phase, γ_1 , proposed by Ref. [1] is likely to be (Li) as shown in Fig. 4.

Fig. 6 shows a wide (Ag) + β two-phase region stable for $0.2 \leq x(\text{Li}) \leq 0.5$ from $298 \leq T(\text{K}) \leq 600$. The homogeneity range of the slightly tetragonal β -phase is wider below 298 K but loses stability progressively, as the temperature increases, while the ordered cubic phase, $\text{AgLi-}\beta$, increases stability up to 600 K. The gamma phase homogeneity range seems to shrink to $x(\text{Li}) = 0.71$ at 425 K in agreement with the phase diagram of Freeth and Reynor [1] (Fig. 4b). The $\text{Ag}_{15}\text{Li}_{49}$ - β is stable from 298 to 425 K. At 600 K, (Ag)- α and $\text{AgLi-}\beta$ are likely to be the only solid phases that are stable.

5. Conclusion

The present studies provide the experimental data for the

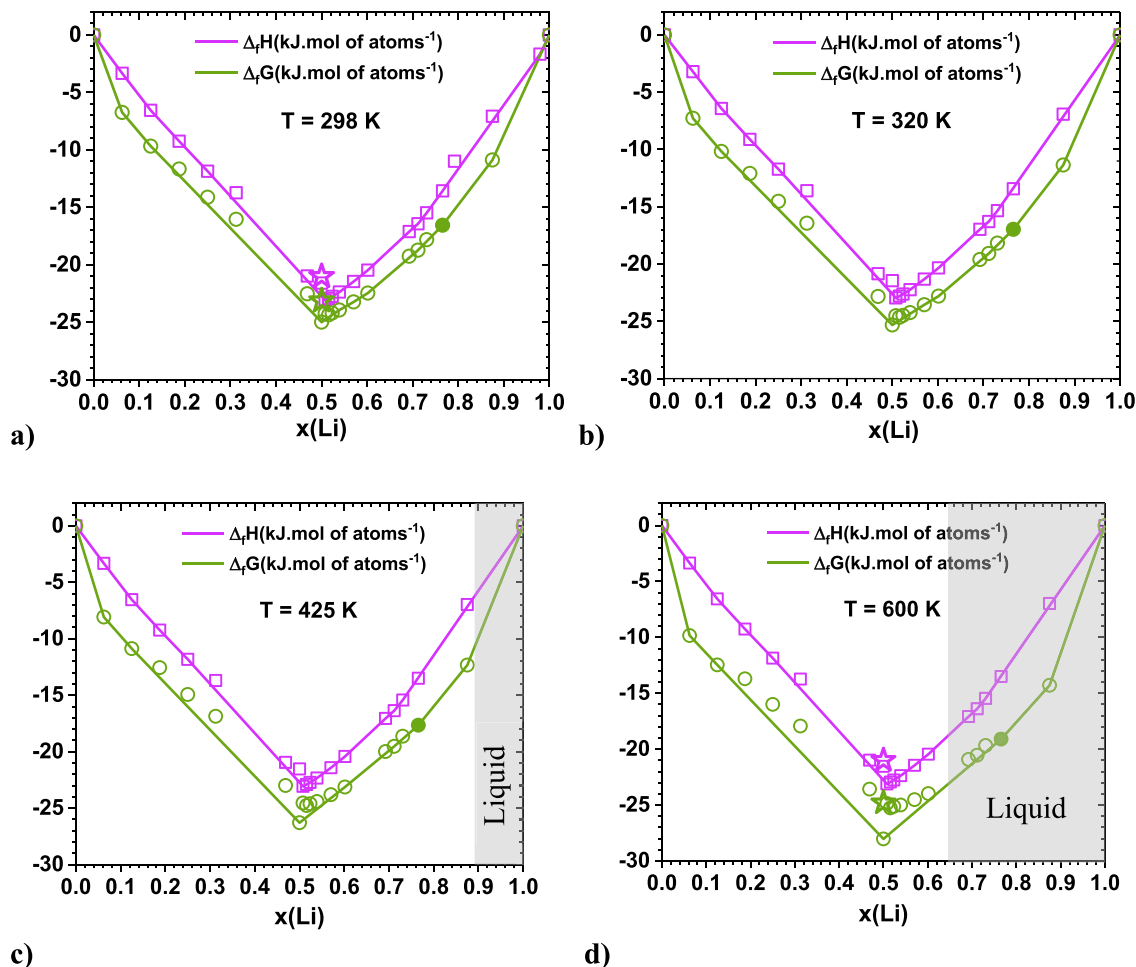
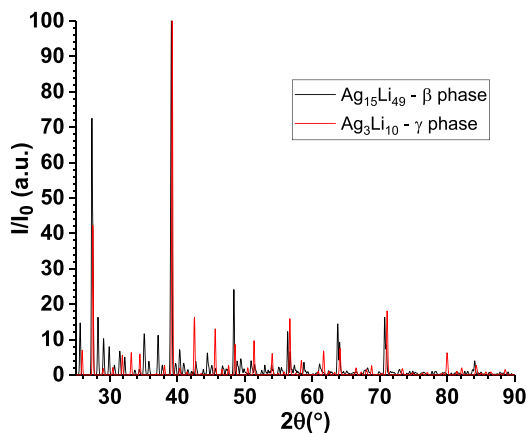


Fig. 6. Enthalpy and Gibbs free energy of formation of Ag–Li intermetallic compounds at different temperatures; a) 298 K; b) 320 K; c) 425 K; d) 600 K. The squares are calculated enthalpies of formation and the circles Gibbs energies of formation (all structures); the star is AgLi , tetragonal sg. $I4_1/amd$ [20], and the full dot is $\text{Ag}_{15}\text{Li}_{49}$ - β_2 which was optimized from a cubic sg, Pm-3m structure.

Table 3

Comparison between experimental and calculated data for the standard enthalpies of formation of the Ag–Li alloys using first principles and Miedema's model [23].

	$\Delta_f H$ [kJ/mol at.]		
	This study by solution calorimetry	First-principles study	Miedema Model [23]
Ag ₅₀ Li ₅₀	–	–23.1	–22.9
Ag ₄₄ Li ₅₆	–	–21.7	–22.9
Ag ₃₀ Li ₇₀	–12.1	–16.8	–18.3
Ag ₂₀ Li ₈₀	–9.0	–11.3	–12.5
Ag ₁₀ Li ₉₀	–6.3	–5.7	–6.2

**Fig. 7.** Calculated XRD patterns for Ag₄₉Li₁₅-β₂ and Ag₃Li₁₀-γ optimized phases.

standard enthalpies of formation of the Ag₃₀Li₇₀, Ag₂₀Li₈₀ inter-metallic gamma phases and for Ag₁₀Li₉₀ alloy corresponding to a hypothetical γ₁ phase measured with the solution calorimetric method. Moreover, the XRD of the Ag₄Li₉-γ disordered phase was obtained and compared with the calculated.

Results indicate that the (Ag) + β region is much wider than expected from the comparison with results in the literature and stable up to 600 K. It was found that the cubic-β phase increases stability with temperature and loses its range of homogeneity to a fixed stoichiometry AgLi-β₁ at 600 K. Only one γ phase was demonstrated to exist, and it is stable for 0.69 ≤ x(Li) ≤ 0.73 at 298 K. A second beta phase, Ag₁₅Li₄₉-β₂ is stable from 298 to 425 K and the third bcc phase, (Li), was found to be stable for 0.91 ≤ x(Li) ≤ 1.00. The γ₁ phase is demonstrated not to exist.

Declaration of competing interest

The authors declare that they have no known competing financial interests or personal relationships that could have appeared to influence the work reported in this paper.

Acknowledgments

The authors want to acknowledge COMPETE2020 and the FCT project PTDC/CTM-ENE/2391/2014.

The authors wish to express their gratitude to the Ministry of

Science and Higher Education of Poland for funding Project No. IP2012 035572 “Thermodynamic research on Ag–Li alloys as a material for safe storage of hydrogen and energy”, financed from the budget for science in the years 2013–2015 and the European Union for the financial support of Project POIG.02.01.00–12–175/09 (Adaptation of the research potential of IMMS PAS to the requirements of the global standards for a comprehensive research in the field of materials science) which enabled the realization of presented investigations with the use of Setaram MHTC 96 Line evo calorimeter.

References

- [1] W.E. Freeth, G.V. Raynor, J. Inst. Met. 82 (1953–54) 569.
- [2] S. Pastorello, Gazz. Chim. Ital. 60 (1930) 493.
- [3] S. Pastorello, Gazz. Chim. Ital. 61 (1931) 47.
- [4] H. Okamoto, Phase Diagram for Binary Alloys, Materials Park, Ohio ASM International, 2000.
- [5] H. Perlitz, Z. Kristallogr. 86 (1933) 155.
- [6] L.D. Firth, N.H.A. Nowaira, W. Scott, J. Phys. F. (Met. Phys.) 4 (1974) L200.
- [7] S.H. Kellington, D. Loveridge, J.M. Titman, J. Phys. D (Appl. Phys. J) 2 (1969) 1162.
- [8] H. Ruppersberg, Phys. Lett. 54A (1975) 151.
- [9] H. Migge, H. Andresen, Scr. Metall. 5 (1971) 175.
- [10] L. Arnberg, S. Westman, Acta Chem. Scand. 26 (1972) 513.
- [11] L. Arnberg, S. Westman, Acta Chem. Scand. 26 (1972) 1748.
- [12] T. Noritake, M. Aoki, S. Towata, T. Takeuchi, U. Mizutani, Acta Crystallogr. B 63 (2007) 726.
- [13] B. Predel, G. Oehme, W. Vogelbein, Z. Metallkd. 69 (1978) 163.
- [14] W. Becker, G. Schwitzgebel, H. Ruppersberg, Z. Metallkd. 72 (1981) 186.
- [15] A.D. Pelton, Bull. All. Phase Diagrams 7 (1986) 223.
- [16] A. Dębski, M.H. Braga, W. Gąsior, J. Chem. Thermodyn. 82 (2015) 53.
- [17] A. Dębski, S. Terlicka, A. Budziak, W. Gąsior, J. Alloy. Comp. 732 (2018) 210.
- [18] W. Gąsior, A. Dębski, J. Chem. Thermodyn. 101 (2016) 270.
- [19] S. Terlicka, A. Dębski, A. Budziak, M. Zabrocki, W. Gąsior, Thermochim. Acta 673 (2019) 185.
- [20] V.V. Pavlyuk, G.S. Dmytriv, I.I. Tarasiuk, I.V. Chumak, H. Pauly, H. Ehrenberg, Solid State Sci. 12 (2010) 274–280.
- [21] J. Wang, P. Chartrand, I.-H. Jung, Calphad 50 (2015) 68–81.
- [22] H. Okamoto, J. Phase Equilibria Diffusion 38 (2017) 70–81.
- [23] F.R. de Boer, R. Boom, W.C.M. Mattens, A.R. Miedema, A.K. Niessen, Cohesion in Metals: Transition Metal Alloys, North-Holland, Amsterdam [etc], 1989.
- [24] W. Gąsior, A. Dębski, A. Góral, R. Major, J. Alloy. Comp. 586 (2014) 703.
- [25] A. Dębski, R. Dębski, W. Gąsior, A. Góral, J. Alloy. Comp. 610 (2014) 701.
- [26] P. Hohenberg, W. Kohn, Phys. Rev. B 136 (1964) 864.
- [27] J.P. Perdew, Y. Wang, Phys. Rev. B 45 (1992) 13244.
- [28] P.E. Blochl, Phys. Rev. B 50 (1994) 17953.
- [29] J.P. Perdew, K. Burke, M. Ernzerhof, Phys. Rev. Lett. 77 (1996) 3865.
- [30] G. Kresse, J. Furthmüller, Phys. Rev. B 54 (1996) 11169.
- [31] MedeA and materials Design. <https://www.materialsdesign.com/> latest consultation Aug. 30th 2019.
- [32] K. Parlinski, Z.Q. Li, Y. Kawazoe, Phys. Rev. Lett. 78 (1997) 4063.
- [33] W. Zakulski, A. Dębski, W. Gąsior, Intermetallics 23 (2012) 76.
- [34] B. Sundman, SGTE SSOL 2.1, ThermoCalc AB, Stockholm, 2002.